THE JOURNAL OF BIOLOGICAL CHEMISTRY
Vol. 279, No. 42, Issue of October 15, pp. 43828–43837, 2004

*Printed in U.S.A.*

# Up-regulation of Neurohemerythrin Expression in the Central Nervous System of the Medicinal Leech, *Hirudo medicinalis*, following Septic Injury*

Received for publication, March 19, 2004, and in revised form, July 14, 2004
Published, JBC Papers in Press, July 16, 2004, DOI 10.1074/jbc.M403073200

**David Vergote‡, Pierre-Eric Sautière‡, Franck Vandenbulcke‡, Didier Vieau‡, Guillaume Mitta§, Eduardo R. Macagno¶, and Michel Salzet‡‖**

*From the ‡Laboratoire de Neuroimmunologie des Annélides, UMR 8017 CNRS, IFR 17 INSERM, Université des Sciences et Technologies de Lille, 59655 Villeneuve d'Ascq, France, the §Centre de Biologie et d'Ecologie Tropicale et Méditerranéenne Parasitologie Fonctionnelle et Évolutive, UMR 5555 CNRS, Université de Perpignan, 66860 Perpignan Cedex, France, and the ¶Section of Cell and Developmental Biology, Division of Biological Sciences, University of California, San Diego, La Jolla, California 92093*

**We report here some results of a proteomic analysis of changes in protein expression in the leech *Hirudo medicinalis in* response to septic injury. Comparison of two-dimensional protein gels revealed several significant differences between normal and experimental tissues. One protein found to be up-regulated after septic shock was identified, through a combination of Edman degradation, mass spectrometry, and molecular cloning, as a novel member of the hemerythrin family, a group of non-heme-iron oxygen transport proteins found in four invertebrate phyla: sipunculids, priapulids, brachiopods, and annelids. We found by *in situ* hybridization and immunocytochemistry that the new leech protein, which we have called neurohemerythrin, is indeed expressed in the leech central nervous system. Both message and protein were detected in the pair of large glia within the ganglionic neuropile, in the six packet glia that surround neuronal somata in each central ganglion, and in the bilateral pair of glia that separate axonal fascicles in the interganglionic connective nerves. No expression was detected in central neurons or in central nervous system microglia. Expression was also observed in many other, non-neuronal tissues in the body wall. Real-time PCR experiments suggest that neurohemerythrin is up-regulated posttranscriptionaly. We consider potential roles of neurohemerythrin, associated with its ability to bind oxygen and iron, in the innate immune response of the leech nervous system to bacterial invasion.**

The nervous system is involved in the control of the major physiological functions leading to homeostasis, including immunity. Kakizaki *et al*. (1) have shown that circulating levels of vertebrate proinflammatory cytokines (tumor necrosis factor-$\alpha$, interleukin-1$\beta$, and interleukin-6) increase upon systemic endotoxemia. Systemic inflammation is detected by brain areas directly in contact with vascular vessels, such as the circumventricular organs, and then spreads to other brain areas. Furthermore, pathogens may trigger an innate immune reaction throughout cerebral tissue without having direct access to the brain parenchyma, leading to the concept of "neuroimmunity" (2). This inflammation triggers double-edged consequences. On the one hand, inflammation in the brain leads to nuclear factor $\kappa$B signaling and transcriptional activation of molecules that engage and control the innate immune response for pathogen elimination. On the other hand, proinflammatory molecules may lead to neurotoxicity and, when bacteria penetrate brain tissue, the release of toxic compounds, like reactive oxygen species, which induce necrosis and apoptosis of both neurons and glial cells.

These observations show that an innate immune response occurs in the vertebrate brain in response to infection with pathogens. In invertebrates, which lack a system for acquired immunity, defenses against invading pathogens rely solely on innate immunity (3, 4), making them very useful models for the identification of pathogen virulence mechanisms and for the study of first line host defense mechanisms (5). Numerous protective mechanisms, humoral as well as cellular, are used by invertebrates for pathogen elimination from the organism. Humoral mechanisms of innate immunity include the release of antimicrobial peptides (6, 7), the production of reactive oxygen or nitrogen species (8, 9), coagulation (10, 11), and the secretion of enzymes that regulate melanization (12). Cellular defenses are based on hemocytic behaviors such as phagocytosis (13), nodulation (14), and encapsulation (15). Insect innate immunity is mainly based on antimicrobial peptides. The discovery of signaling pathways regulating their production as well as the pattern recognition receptors implicated in their activation (16) have greatly contributed to a better understanding of the key role of the innate immune response in vertebrates and its conservation in course of evolution.

Molecules playing a role in innate immunity in peripheral organs (*e.g.* the fat body in insects) and in circulating fluids (blood or coelomic fluid) (6) are also found in the nervous system. Indeed, lectin family proteins (17) and the Rel family member *Dif* and the I$\kappa$B molecule *Cactus*, known as transcriptional regulators of several antimicrobial peptides, have been co-localized in the larval nervous systems of *Drosophila mela-*

* This work was supported in part by the Centre National de la Recherche Scientifique, the Ministère de l'Education Nationale, de la Recherche et des Technologies, the Fond Economique du Développement Européen et Régional, the Conseil Régional Nord-Pas-de-Calais, the Génopôle de Lille, the Plateau de Protéomique de l'Université des Sciences et Technologies de Lille, and the National Institutes of Health-Fogarty Grant. The costs of publication of this article were defrayed in part by the payment of page charges. This article must therefore be hereby marked "*advertisement*" in accordance with 18 U.S.C. Section 1734 solely to indicate this fact.

*The nucleotide sequence(s) reported in this paper has been submitted to the GenBank™/EBI Data Bank with accession number(s) AY521548 (for the nucleotide and amino acid sequences for neurohemerythrin gene and protein).*

‖ To whom correspondence should be addressed. Tel.: 33-3-20-43-68-39; Fax: 33-3-20-43-40-54; E-mail: michel.salzet@univ-lille1.fr.

*nogaster* (18). Several Toll-like receptors have also been found in neuronal or glial cells of insects and nematodes (19, 20). All these proteins have been shown to play crucial roles in the neural development, but it is not yet clear whether they also have roles in innate immunity within the nervous system except for the *tol-1* gene product of *Caenorhabditis elegans* expressed in pharyngeal neurons and involved in avoidance of pathogenic bacteria ingestion (20).

Innate immunity mechanisms are less known in annelids than in insects and nematodes. Most studies of annelid defenses have reported the isolation of molecules based on their biological activities, such as antimicrobial (21) or pattern recognition receptor properties (22), or on their homologies with vertebrate molecules (23, 24), without careful analyses of the mechanisms involved. Among annelids, one of the best known species is the medicinal leech, *Hirudo medicinalis*, which has been intensively studied since the XIX° century (25, 26). Its central nervous system is by now very well described, with some 400 neurons per segmental ganglia, most of them identified and characterized morphologically and physiologically (27). The development of the nervous system and its capacity to regenerate accurate synaptic connections after nerve damage are also well documented (28–31). Because so much is already known about the properties of the normal embryonic and adult CNS, the medicinal leech is an excellent system for the investigation of the mechanisms of the neuronal response to bacterial challenge.

Using a global approach based on two-dimensional gel electrophoresis, we have investigated whether the central nervous system of the leech *H. medicinalis* responds to bacterial challenge with detectable changes in its profile of protein expression. We report here that, among several significant observable changes, the leech nervous system responds to bacterial challenge by increasing the translation of a member of the Hemerythrin family of oxygen-carrying proteins.

## EXPERIMENTAL PROCEDURES

*Animals*—Adult *Hirudo medicinalis* specimens were obtained from Ricarimpex (France) and kept in artificial pond water for acclimatization for at least 1 week before being used in experiments.

*Two-dimensional Gel Electrophoresis—H. medicinalis* central nervous systems were dissected out in leech Ringer (115 mM NaCl, 1.8 mM $CaCl_2$, 4 mM KCl, 10 mM Tris maleate, pH 7.4), bathed for *ex vivo* septic shock in $2 \times 10^8$ bacteria from a mixture of Gram-positive and negative bacteria (*Escherichia coli/Micrococcus luteus*) or in phosphate-buffered saline for 6 h before being frozen in liquid nitrogen. Batches of 10 control or experimental central nervous systems were stored prior to molecular analysis at −80 °C.

The initial steps in protein extraction consisted of three freezing/defrosting cycles, ultrasonic extraction, and 10% trichloroacetic acid/acetone precipitation. Dried pellets were then incubated 2 h at room temperature in "lysis" buffer (9.5 M urea, 2% Triton X-100, 65 mM β-mercaptoethanol, 1.25% SDS) (32). The protein concentration of each sample was determined using the Peterson method (33).

Isoelectrofocusing for the two-dimensional gel electrophoresis was performed with the IEFCell system (Bio-Rad). Immobilized pH 3–10 linear gradient strips were rehydrated in a reswelling solution containing 9 M urea, 2% Triton X-100, 10 mM dithiothreitol (DTT),[1] 0.2% v/v Bio-lyte, pH 3–10:pH 5–8:pH 7–9, 1:1:2 (Bio-Rad) and 350 μg or 1 mg of proteins from the nervous system of *H. medicinalis* (for analytical or preparative electrophoresis, respectively). Rehydration was passive for 6 h, then active at 50 V for 14 h at 20 °C. Isoelectrofocusing voltage was rising gradually until 8000 V and running until 180,000 V·h at 20 °C. After focusing, the strips were incubated with 130 mM DTT in equilibration buffer (6 M urea, 375 mM Tris-HCl, 2% SDS, 20% glycerol, 0.02% Coomassie Blue G-250, pH 8.8) twice 15 min to reduce the proteins according to Wu *et al.* (34). Then the proteins were carbamidomethylated for a further 15 min with 135 mM iodoacetamide in equilibration buffer.

The immobilized pH 3–10 linear gradient strips were transferred on a 12% polyacrylamide gel containing 0.8% of cross-linker piperazine diacrylamide. Electrophoresis was performed in Tris/Tricine buffer according to the conditions defined by Schägger and von Jagow (35). Proteins were running 1 h at 30 V and then at 150 V until Coomassie Blue reached the bottom of the gel. After electrophoresis, gels were silver-stained according to a modified protocol of Morrissey (36) for Coomassie Blue stain according to Neuhoff (37).

*Two-dimensional Image Analysis*—Four gels per condition were analyzed using the Progenesis™ v1.5 software program (Nonlinear dynamics, Newcastle upon Tyne, UK). The analysis protocol included spot detection and filtering, whole image warping on a reference gel, background subtraction, average gel creation, spot matching, and volume normalization against the total volume of all protein spots present in the gel. Each analysis step was manually validated. In creating the gel average, one spot absence in the gel series was allowed. Statistical significance was measured by Student's paired *t* test.

*Edman Degradation*—Two-dimensional spots were excised and eluted according to Shaw (38) from Coomassie Blue-stained electrophoresis gels. $NH_2$-terminal amino acid sequencing was performed on a pulse-liquid automatic peptide PerkinElmer Life Sciences/Applied Biosystems Procise cLC-492 microsequencer.

*In-gel Digestion for Mass Spectrometry Analysis*—Polyacrylamide gel pieces of Coomassie Blue-stained proteins were washed in 25 mM ammonium bicarbonate, 50% acetonitrile. After drying, they were placed on ice for 30 min in 50 μl of protease solution (sequence grade-modified trypsin, Promega, at 0.02 mg/ml in 25 mM ammonium bicarbonate). Excess of protease solution was then removed and replaced by 50 μl of 25 mM ammonium bicarbonate. Digestion was performed overnight at 30 °C. Peptide extraction was performed twice 15 min with 50% acetonitrile, 1% trifluoroacetic acid for further MALDI-MS analysis or with 50% acetonitrile, 1% formic acid for further ESI-MS-MS analysis. Trypsin digests were then lyophilized in a SpeedVac concentrator (Savant) and resuspended in 5 μl of 0.1% trifluoroacetic acid or 0.1% formic acid.

*Matrix-assisted Laser Desorption/Ionization-Time of Flight Mass Spectrometry (MALDI-TOF MS)*—MALDI-TOF MS analysis of trypsin digests was performed on a Voyager DE Pro (Applied Biosystems) in reflector mode at an accelerating voltage of 20 kV. One microliter of trypsin digests was spotted on 1 μl of dried α-cyano-4-hydroxycinnamic acid, 15 mg/ml in acetone and covered with 1 μl of α-cyano-4-hydroxycinnamic acid (10 mg/ml) in 70% acetonitrile, 0.1% trifluoroacetic acid. About 300 laser shots were accumulated to obtain the final spectrum. Mass measurements were then finalized after peak smoothing and internal calibration using the two autolysis trypsin fragments 2211.1 and 842.51. Protein data base searching was performed using MS-Fit (prospector.ucsf.edu/ucsfhtml4.0/msfit.htm) according to the monoisotopic molecular weight of $[M+H]^+$ peptides ions.

*ESI-MS/MS Analysis*—After desalting the samples on a C18 Zip-Tip (Millipore, Bedford, MA), the samples were loaded into nanoES capillaries (Protana, Odense, Denmark) using a 5-μl on-column syringe. The capillaries were inserted into an Applied Biosystems Q-STAR Pulsar (Q-TOF-MS) using an ion spray source. Doubly charged peptides were selected, fragmented by $N_2$ collision, and analyzed by MS-MS. The MS-MS sequence was manually assigned to search against Swiss-Prot, NCBI, and GenPept using Fasts software (fasta.bioch.virginia.edu/fasta_www/cgi/search_frm.cgi?pgm=fs) (39).

*Cloning and Sequencing*—Total RNA extraction was performed with the TRIzol® kit (Invitrogen) according to manufacturer's conditions. First-strand cDNAs were prepared from these total RNAs with oligo$(dT)_{12-18}$ for primer. Five micrograms of RNA were first denatured 10 min at 70 °C in the presence of 2 μl of 100 μM primer in a total volume of 26.5 μl. First-strand synthesis was generated in a 40-μl volume by adding 2 μl of deoxynucleotide triphosphate (dNTP) at 10 mM, 1 μl of RNase inhibitor, 1 μl of 0.1 M DTT, 8 μl of 5× buffer (250 mM Tris-HCl, pH 8.3, 375 mM KCl, 15 mM $MgCl_2$), and 1.5 μl of Superscript II™ (200 units/μl, Invitrogen). Incubation was performed for 55 min at 42 °C, then RNA was hydrolyzed at 55 °C for 15 min in the presence of 1 μl of RNase H. To clone the 5′-end of the cDNA, we added a poly(A) tail to the cDNA first strand. For this, 8 μl of cDNA were mixed with 2 μl of 5× buffer, 2 μl of 2 mM ATP, and 1 μl of terminal deoxynucleotide transferase (Invitrogen) in a total volume of 20 μl. The mixture was incubated 15 min at 37 °C followed by 10 min at 65 °C.

PCRs were performed in 50-μl mixtures containing 2 μl of first-strand cDNA as a template in PCR buffer 1× (Q-Biogene), 1 μl of

[1] The abbreviations used are: DTT, dithiothreitol; ESI-MS-MS, electrospray ionization-tandem mass spectrometry; MALDI-TOF MS, matrix-assisted laser desorption/ionization-time of flight mass spectrometry; CP, crossing point; Tricine, *N*-[2-hydroxy-1,1-bis(hydroxymethyl)ethyl]glycine.

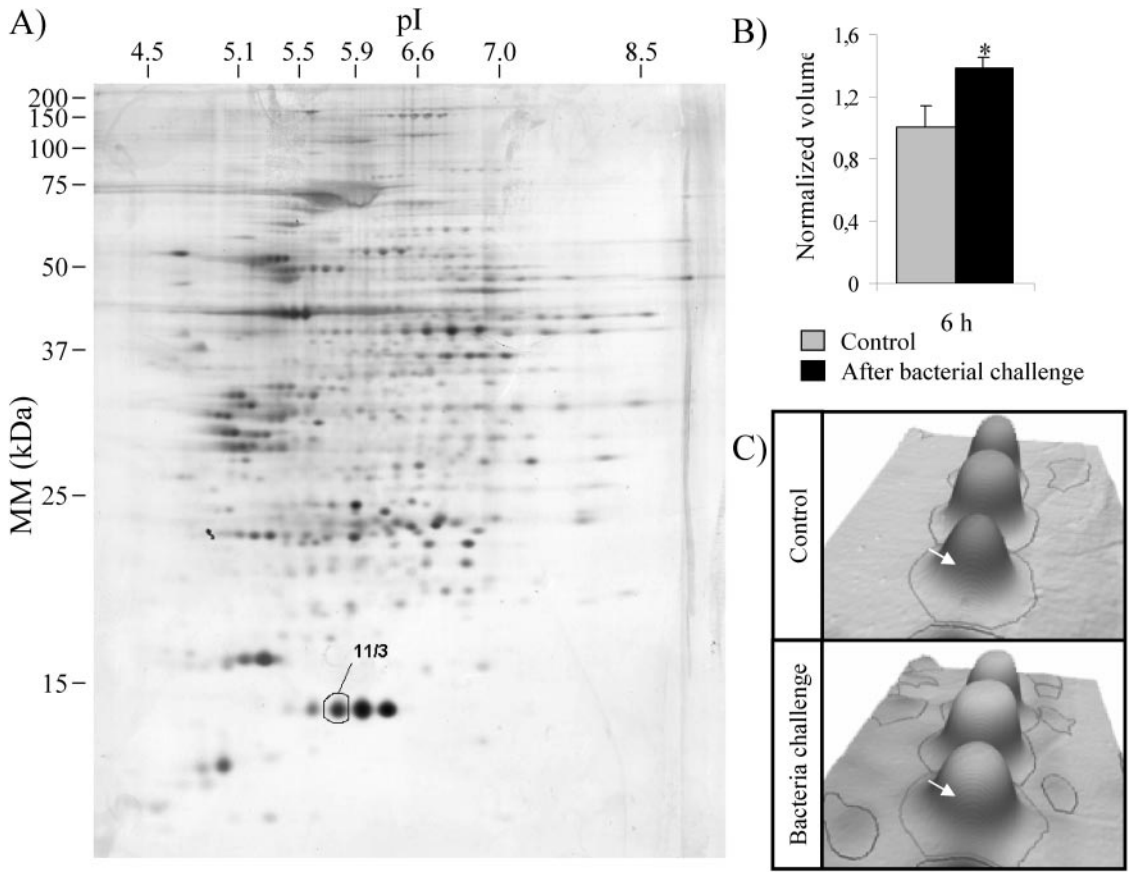


FIG. 1. **Modification of the expression of the 11/3 protein spot following sepsis.** *A*, silver-stained two-dimensional gels of *H. medicinalis* nerve cords. Molecular mass (*MM*) calibration is indicated on the *left* of the gel and pI calibration on the *top* of the gel. Note that the pI calibration is approximate, since the pI standards had to be run separately from the isoelectrofocusing gel strip. The 11/3 protein is *circled*. *B*, the expression of the 11/3 protein increases in nerve cords following bacterial challenge. Expression measurements were made with Progenesis™ software. The figure shows the averaged results from four gels for each condition. The increase is significant (*, $p < 0.05$). *C*, three-dimensional view of the 11/3 spot in control and bacteria challenge conditions.

primer, and 1 $\mu$l of oligo d(T)$_{12-18}$, each dNTP at 200 $\mu$M, and 1 unit of TaqDNA polymerase (PerkinElmer Life Sciences). The PCR condition involves initial heating at 94 °C for 5 min followed thereafter by 30 cycles of denaturation at 94 °C for 40 s, primer annealing at 50 °C for 1 min, and primer extension at 72 °C for 1 min. Amplification cycles were followed by a final extension at 72 °C for 7 min. PCRs were performed in an Eppendorf Mastercycler gradient. The final PCR mixtures were analyzed on 1% (w/v) agarose gel.

The PCR products were ligated into the pGEM-T easy vector according to the manufacturer's instructions (Promega). Dideoxy sequencing reactions of the recombinant plasmids were analyzed with the T7 sequencing kit from Amersham Biosciences. The nucleotide sequences were analyzed on an ABI Prism® 310 Genetic Analyzer (Applied Biosystems).

*Real-time PCR*—Reverse transcription was performed as described above. Specific forward and reverse primers were designed using the LightCycler Probe Design software (Roche Applied Science), based on sequence data from the hemerythrin nucleic acid sequence. The primer sequences were: HEMF1 5′-TTCAGGCTTCTCTCGG-3′ and HEMR1b 5′-GTCAACTTCGACAAATCTGC-3′. Primers for the control gene were designed from the sequence of a protein of the large ribosomal subunit available in a *H. medicinalis* expressed sequence tag data base: RPL7-aF2, 5′-AATGATGAGGTCAGGCA-3′; RPL7aR2b, 5′-GGATCTCTTCA-GCCCTTT-3′. PCRs were set up according to the LightCycler manual (Roche Applied Science). A mastermix of the following reaction components was prepared as follows (final concentrations): 8.6 $\mu$l of water, 2.4 $\mu$l of $MgCl_2$ (4 mM), 1 $\mu$l of forward primer (0.4 $\mu$M), 1 $\mu$l of reverse primer (0.4 $\mu$M), and 2 $\mu$l of LightCycler Fast Start DNA Master SYBR Green I (Roche Diagnostics). LightCycler mastermix (15 $\mu$l) was filled in the LightCycler glass capillaries, and 5 $\mu$l of cDNA was added as PCR template. All primers were highly purified and salt-free (40). The following LightCycler run protocol was used: denaturation program (95 °C, 10 min), amplification and quantification programs repeated 40 times (95 °C for 15 s, annealing temperature for 5 s, 72 °C for 13s), melting curve program (60–95 °C with a heating rate of 0.1 °C/s and continuous fluorescence measurement), and a cooling step to 40 °C. Analysis of melting curves allowed optimization of annealing temperatures for each amplification product. Single highly specific amplification products were obtained using annealing temperatures ranging from 1 °C below to 1 °C above the $T_m$ of primer pairs. For each reaction, the crossing point (CP) (defined as the cycle number at which the noise band intersects the fluorescent curves) was determined using the "Fit Point Method" of the LightCycler software 3.3 (Roche Diagnostics). PCRs were all set in triplicate, and the mean value of the three CPs was calculated. Intra-assay variation (test precision) of CPs was assessed by the coefficient of variation = (S.D. ± mean) × 100 (40, 41). In addition, a no-template control ($H_2O$ control) was analyzed for each mastermix.

To calculate amplification efficiencies ($E$) of each target cDNA, relative standard curves were generated using serial dilutions (1, 1:10, 1:50, 1:100, 1:500, and 1:1000) of a unique leech nervous system cDNA sample consisting of a pool of the three cDNAs to be analyzed (1:1:1). Standard curves were generated by the LightCycler software. They are based on the values of CPs and the log value of the standard cDNA dilution. Real-time PCR efficiencies ($E$) were calculated from the given slope of the standard curve according to the equation $E = 10^{(-1/\text{slope})}$. For each sample, the level of expression of the target gene was compared with the expression of a large subunit ribosomal gene. As amplification efficiencies for each sample were 2, the expression ratio ($R$) is calculated according to the formula $R = 2(CP_{\text{ribosomal}} - CP_{\text{hemerythrin}})$.

*In Situ Hybridization*—A plasmid containing the 3′-end (641 bp) of hemerythrin was used as a template for the preparation of the probes. Digoxigenin-11-UTP and $^{35}$S-UTP-labeled antisense and sense riboprobes were generated from linearized cDNA plasmids by *in vitro* transcription using RNA labeling kits (Roche Applied Science) and $^{35}$S-UTP (Amersham Biosciences).

Total animals or isolated nerve cords of *H. medicinalis* were fixed 2 h in a solution containing 4% paraformaldehyde in 0.1 M phosphate buffer, pH 7.4. After dehydration, tissues were embedded in Paraplast,

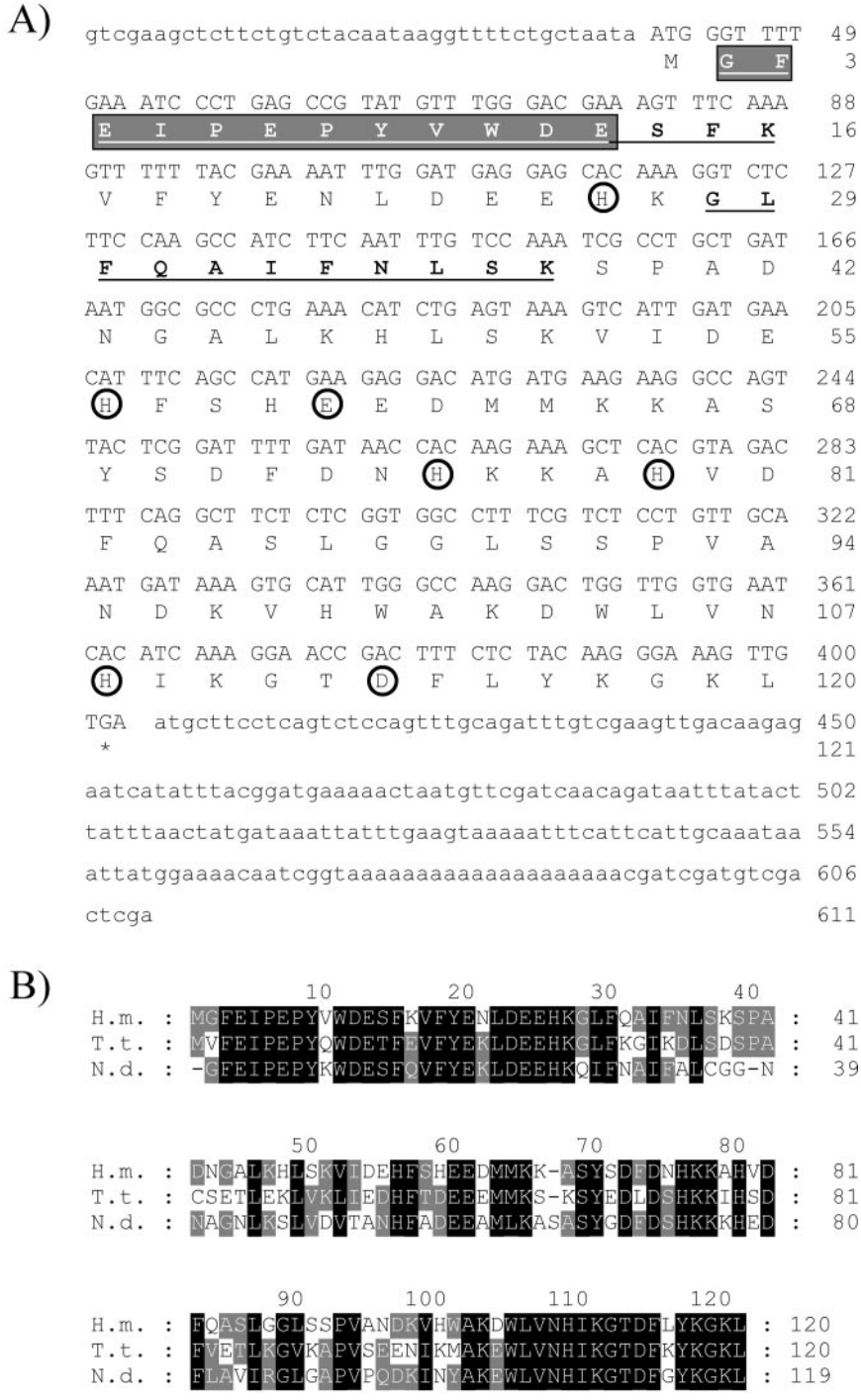


FIG. 2. **Sequence analysis of hemerythrin.** *A*, determined nucleotide and predicted amino acid sequences of *H. medicinalis* hemerythrin. Nucleotides and amino acid residues are numbered on the *right*. An *asterisk* denotes the stop codon, and the polyadenylation signal (aataaa) is *underlined*. The seven residues involved in iron binding in hemerythrin are *circled*. The $NH_2$-terminal sequence obtained by Edman degradation is shown with a *darker gray background*, and the sequence obtained by ESI-MS-MS is shown in *bold* and *underlined*. *B*, sequence alignment of hemerythrin from *H. medicinalis* and *T. tessulatum* (NCBI Q9GYZ9) and the hemerythrin-like protein MPII of *N. diversicolor* (NCBI P80255).

and 8-$\mu$m sections were cut, mounted on poly-L-lysine-coated slides, and stored at 4 °C until use.

Digoxigenin-labeled riboprobes (40–100 ng per slide) and $^{35}$S-labeled riboprobes (100 ng or $10^6$ counts/min per slide) were hybridized to tissue sections as described previously (42, 43). Riboprobes were diluted in hybridization buffer containing 50% formamide, 10% dextran sulfate, 10× Denhardt's solution, 0.5 mg/ml tRNA from *E. coli*, 100 mM DTT, and 0.5 mg/ml salmon sperm DNA. Hybridization was carried out overnight at 55 °C in a humid chamber. Slides were then washed twice (2 × 30 min) with 2× SSC (standard saline citrate), treated with RNase A (20 $\mu$g/ml in 2× SSC) for 30 min at 37 °C, and consecutively rinsed twice for 30 min at 55 °C. The probes labeled with digoxigenin-UTP were revealed using alkaline phosphatase-conjugated antibodies as described previously (42).

The $^{35}$S-UTP hybridization signal was visualized using autoradiography. Samples were coated by dipping in LM1 Amersham liquid emulsion, immediately dried, and exposed for a 10-day period. At the end of the exposure period, the autoradiograms were developed in D19b (Eastman Kodak Co.), fixed in 30% sodium thiosulfate (10 min at room temperature), stained with toluidine blue, and mounted with XAM mounting medium (Merck).

Slides were observed under a Zeiss Axioskop microscope, and images were captured with a system equipped with the Leica IM 1000 software.

Controls for *in situ* hybridization consisted of replacing antisense riboprobe with sense riboprobe. RNase control sections were obtained by adding a preincubation step with 10 $\mu$g/ml RNase A prior to hybridization.

*Immunocytochemistry*—A potentially immunogenic region of hemerythrin (HIKGTDFKYKGKL) (His$^{108}$–Leu$^{120}$) was chemically synthesized, coupled to ovalbumin, and then used to immunize two New

**A)**

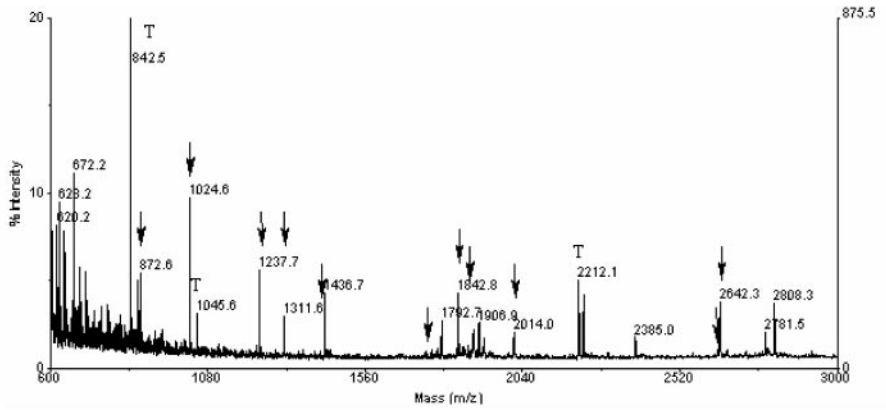


**B)**

| $[M+H]^+_{exp}$ | $[M+H]^+_{th}$ | Δppm | Covered residues | Sequence |
|---|---|---|---|---|
| 872,45 | 872,45 | 0 | 39-47 | (K) SPADNGALK (K) |
| 1024,56 | 1024,56 | 0 | 103-110 | (K) DWLVNHIK (G) |
| 1237,68 | 1237,69 | -8 | 28-38 | (K) GLFQAIFNLSK (S) |
| 1311,59 | 1311,60 | +8 | 66-76 | (K) KASYSDFDNHK (K) |
| | | | 67-77 | (K) ASYSDFDNHKK (A) |
| 1422,64 | 1422,65 | -7 | 17-27 | (K) VFYENLDEEHK (G) |
| 1746,72 | 1746,75 | -17 | 52-65 | (K) VIDEHFSHEEDMMK (K) |
| 1842,85 | 1842,70 | +81 | 2-16 | (M) GFEIPEPYVWDESFK (V) |
| 1874,86 | 1874,84 | +11 | 52-66 | (K) VIDEHFSHEEDMMKK (A) |
| 2012,99 | 2013,00 | -5 | 78-97 | (K) AHVDFQASLGGLSSPVANDK (V) |
| 2634,32 | 2634,34 | -8 | 78-102 | (K) AHVDFQASLGGLSSPVANDKVHWAK (V) |
| 2641,34 | 2641,33 | +4 | 17-38 | (K) VFYENLDEEHKGLFQAIFNLSK (S) |

FIG. 3. **Peptide mass fingerprint of the 11/3 protein.** *A*, MALDI-TOF mass spectrum, acquired in the reflectron mode, of *H. medicinalis* hemerythrin after digestion with modified trypsin, as described under "Experimental Procedures." *Arrows* indicate tryptic fragments corresponding to theoretical digestion of the sequence presented in Fig. 2. *T* indicates the autodigested fragment of trypsin. *B*, comparison of experimental tryptic fragment masses of the 11/3 protein (*column 1*) and tryptic fragment masses predicted theoretically from the sequence of *H. medicinalis* hemerythrin (*column 2*).

Zealand rabbits according to the protocol of Agrobio (La Ferté St Aubin, France) to recover antisera.

Tissue sections obtained as decribed above were preincubated 1 h in TBS (0.1 M Tris, pH 7.4, 0.9% NaCl) containing 1% normal goat serum, 1% ovalbumin, and 0.05% Triton X-100. Then, sections were incubated overnight at 20 °C in TBS containing 1:400 rabbit anti-hemerythrin antiserum, 1% normal goat serum, 1% ovalbumin, 0.05% Triton X-100. After washes in TBS, sections were incubated for 2 h with a goat anti-rabbit fluorescein isothiocyanate-tagged antiserum (Jackson ImmunoResearch) diluted 1:100 in TBS. After washes, slides were mounted in glycerol containing 25% TBS and 0.1% *p*-phenylenediamine. Labeled cells were observed using a Leica laser scanning microscope (TCS NT) equipped with a Leica (DMIRBE) inverted microscope and an argon/krypton laser. Fluorescein isothiocyanate signal was detected using a 488 nm band pass excitation filter and a 575–640 nm pass barrier filter. Images were acquired sequentially as single transcellular optical sections and averaged over 16 scans/frame.

Controls consisted of incubations of anti-hemerythrin immunserum preadsorbed with the $His^{108}$–$Leu^{120}$ synthesis peptide.

## RESULTS

*Neurohemerythrin Is Up-regulated following Sepsis*—Proteins from leech nervous systems, normal or subjected to sepsis, were separated by two-dimensional gel electrophoresis and stained with silver nitrate for image gel analysis using Progenesis™ software. The two-dimensional electrophoretic profile of leech nervous system proteins is illustrated in Fig. 1*A*.

Among the changes observed as a result of sepsis, the increase in the signal of the spot labeled 11/3 was particularly noticeable and was chosen for further analysis. A quantitative assay of the size of the signal (see "Experimental Procedures") revealed that the change in the annotated protein spot 11/3 was significant ($p < 0.05$; Student's paired $t$ test). The normalized volume of this protein spot, which corresponds to a protein of about 14–15 kDa and a pI between 5 and 6 (Fig. 1*A*), increased by about 40% over controls following bacterial challenge (Fig. 1*B*).

To identify the 11/3 protein, we first performed an in-gel digestion with trypsin, followed by MALDI-TOF mass spectrometry analysis. This yielded a peptide mass fingerprint for the 11/3 protein, but this was insufficient information for the immediate identification of the protein because of the current lack of detailed genomic sequence information for the *H. medicinalis* genome. After passive elution, followed by Edman sequencing, we obtained the 12 $NH_2$-terminal amino acids of the protein. This sequence, $H_2N$-GFEIPEPYVWDE . . . , was then compared with those in the Swiss-Prot and NCBI databases using the MS-Pattern program (prospector.ucsf.edu/ucsfhtml4.0/mspattern.htm). The comparisons with the two data bases yielded the same identification, a hemerythrin family protein, a divalent cation-binding protein already described in two other Annelids, the sand worm *Nereis diversicolor* (NCBI P80255; 92% identity) and the rhynchobdellid leech *Theromyzon tessulatum* (NCBI Q9GYZ9; 83% identity) (44, 45).

To obtain sequence tags, tryptic digests of the 11/3 protein were analyzed on a Q-TOF-MS. ESI-MS-MS experiments on two tryptic fragments gave two sequence tags $H_2N$-GFEL′PE-

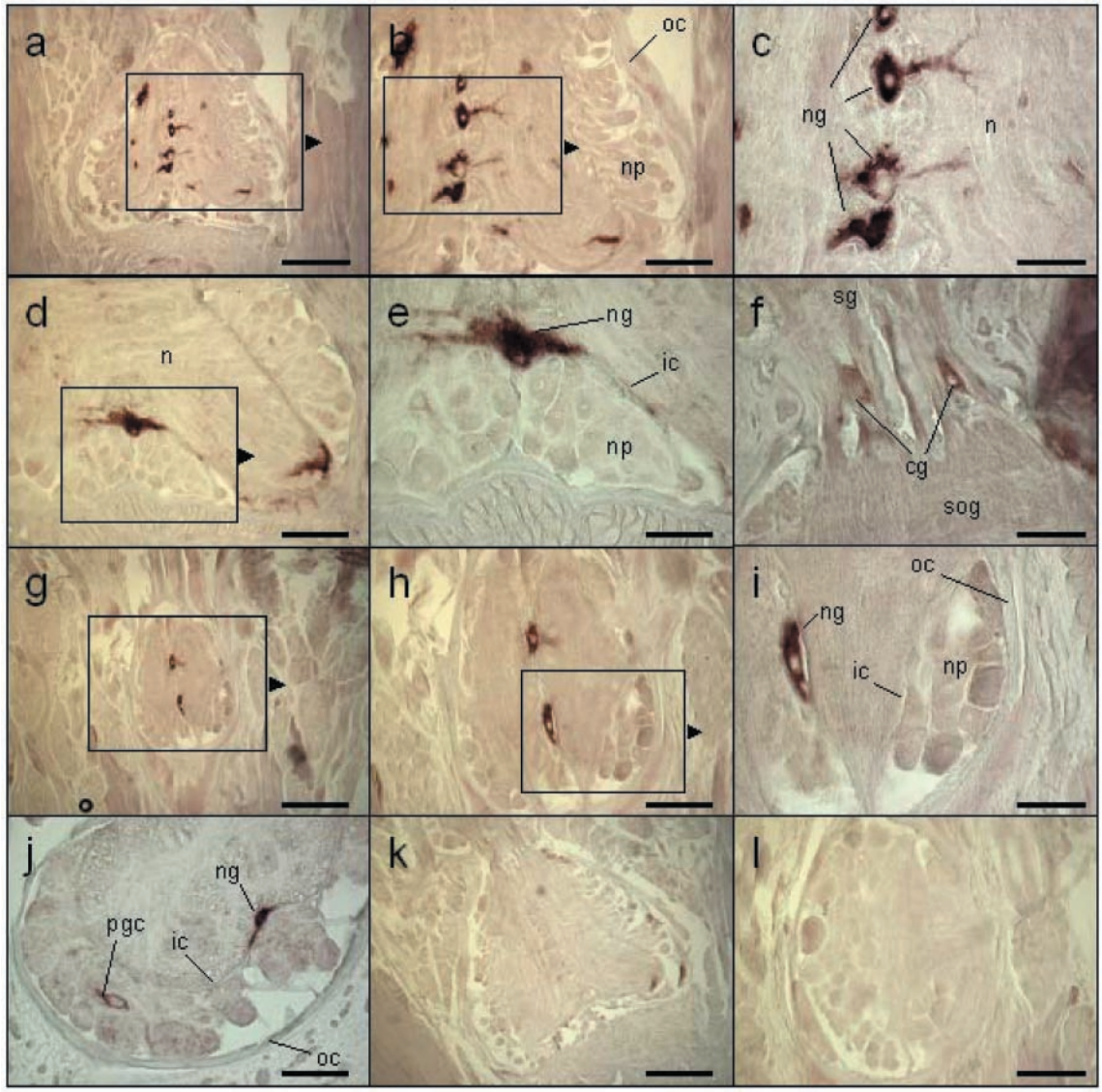


FIG. 4. **Detection of hemerythrin message in the CNS of *H. medicinalis*.** Sections were hybridized with digoxygenin-labeled RNA probes, followed by immunodetection as described under "Experimental Procedures." *a–e*, antisense hemerythrin probe labeling in head ganglia. *g–j*, antisense hemerythrin probe labeling in segmental ganglia. *f*, antisense hemerythrin probe labeling in connectives between segmental ganglia. *k*, sense hemerythrin probe labeling in head ganglion. *l*, sense hemerythrin probe labeling in segmental ganglia. *cg*, connective glia; *ic*, inner capsule; *n*, neuropile; *ng*, neuropile glia; *np*, neuronal packet; *oc*, outer capsule; *pgc*, packet glial cell; *sg*, segmental ganglia; *sog*, suboesophageal ganglion. *Scale bars*: 40 $\mu$m (*a*, *g*, and *k*), 20 $\mu$m (*b*, *d*, *f*, *j*, and *l*), and 10 $\mu$m (*c*, *e*, and *i*).

PYVWDESK-COOH (covering the sequence obtained by Edman degradation) and $H_2N$-GL′FZAL′FNL′SK-COOH (where L′ could be I or L and Z, Q, or K, respectively). The second sequence obtained by ESI-MS-MS was used to design oligonucleotide primers. The two primers designed were: 5′-A-AGGGIHTITTYCARGC-3′ for the sense primer and 5′-GATN-GCYTGRAAIADICC-3′ for the antisense primer. Using two sets of primers, the sense primer and oligo$(dT)_{12–18}$ on cDNA and the antisense primer and oligo$(dT)_{12–18}$ on cDNA with a poly(A) tail added, we isolated and sequenced two clones. The combined sequence of the two clones allowed us to obtain the complete sequence of *H. medicinalis* hemerythrin. This hemerythrin cDNA is 613 bp in length (Fig. 2*A*) and encodes a 120-amino acid residue protein. The deduced protein has a calculated monoisotopic mass of 13,674.7 Da and a theoretical pI of 6.39, not including any posttranslational modifications. The amino acid sequence showed 66 and 62% identity with *N. diversicolor* and *T. tessulatum* hemerythrin, respectively (Fig. 2*B*). The predicted protein contains the hemerythrin signature sequence (PROSITE, PS 00550) and all of the residues involved in iron binding in sipunculid hemerythrins (46, 47), namely $His^{26}$, $His^{56}$, $Glu^{60}$, $His^{75}$, $His^{79}$, $His^{108}$, and $Asp^{113}$ (Fig. 2) were strictly conserved. Theoretical tryptic fragments of the amino acid sequence deduced from the cloned *H. medicinalis* hemerythrin were compared with the peptide mass fingerprint obtained after tryptic digestion of the protein 11/3. Eleven common fragments were identified. These 11 fragments covered 88% of the deduced amino acids sequence of the protein (Fig. 3). Thus, Edman sequencing, cDNA cloning, and mass spectrometry brought proof of the 11/3 protein identification as a hemerythrin family member. As described below, this protein is expressed in the nervous system, as well as other tissues, and hence we have named it neurohemerythrin.

*Neurohemerythrin Is Regulated Posttranscriptionally*—To investigate the up-regulation level of hemerythrin under bacterial challenge, we have evaluated hemerythrin transcript population against a ribosomal transcript using real-time reverse transcription-PCR. Calculation of expression ratios (data not shown) showed that hemerythrin transcription is not significantly modulated between control and septic con-

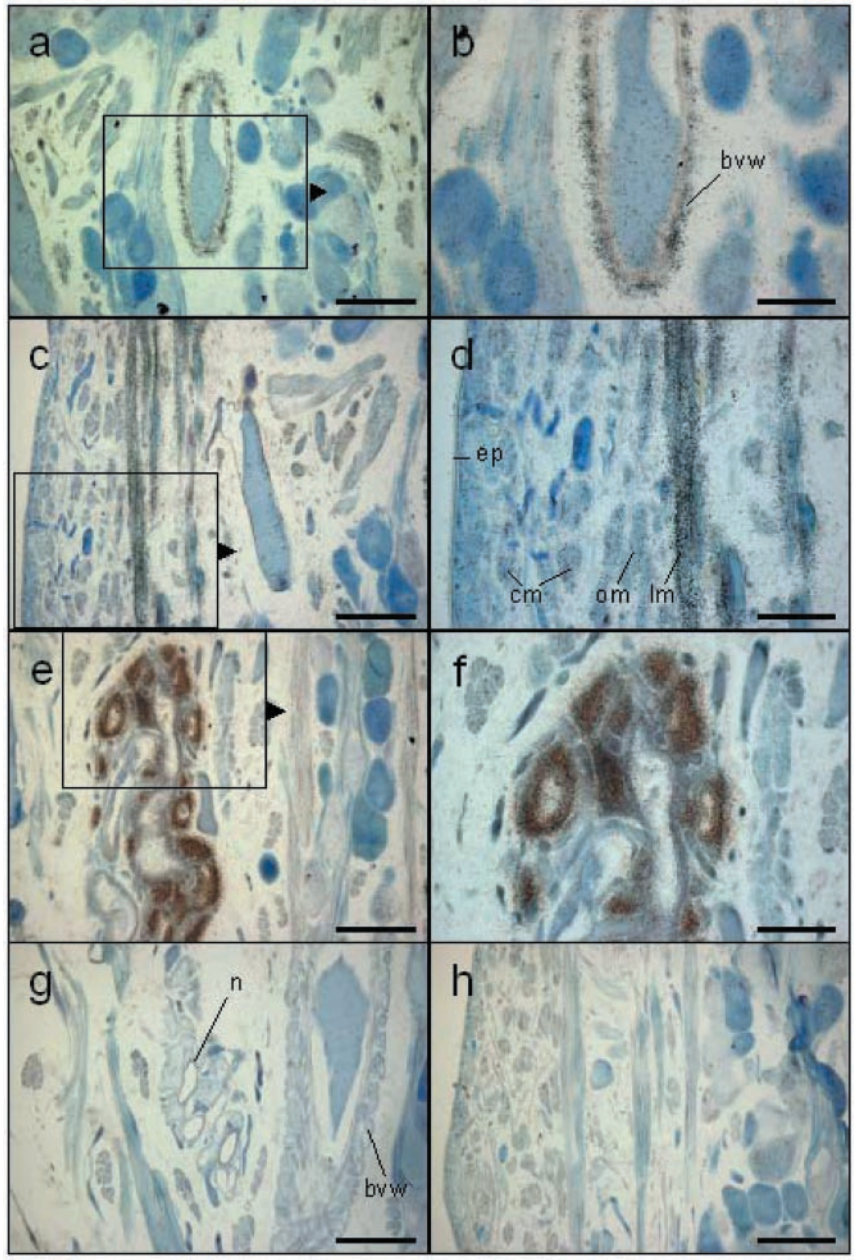


FIG. 5. **Detection of hemerythrin messages in peripheral structures of *H. medicinalis*.** Sections were hybridized with $^{35}$S-labeled RNA probes as described under "Experimental Procedures." *a* and *b*, antisense hemerythrin probe labeling in blood vessel wall. *c* and *d*, antisense hemerythrin probe labeling in muscle. *e* and *f*, antisense hemerythrin probe labeling in nephridia. *g* and *h*, sense hemerythrin probe labeling in blood vessel wall and nephridia and in muscles, respectively. *bvw*, blood vessel wall; *cm*, circular muscles; *ep*, epidermis; *lm*, longitudinal muscles; *n*, nephridia; *om*, oblique muscles. *Scale bars*: 40 $\mu$m (*a*, *c*, *e*, *g*, and *h*) and 20 $\mu$m (*b*, *d*, and *f*).

ditions after 2 h of incubation nor after 6 h. These results suggest that up-regulation of hemerythrin occurs at a post-transcriptional level.

*Neurohemerythin Is Expressed by Glial Cells in the CNS as Well as Various Cells in Peripheral Tissues*—Hemerythrin mRNA was detected in paraffin sections of adult leech tissues by *in situ* hybridization with digoxigenin- or $^{35}$S-labeled antisense riboprobes, with a sense probe providing a control for specificity. Signal was detected both in the nervous system (Fig. 4) and in peripheral tissues (Fig. 5). As mentioned above, the expression in the nervous system has led us to call the hemerythrin molecule we identified neurohemerythrin.

In the leech CNS, as in other invertebrates, the neuronal cell bodies in each ganglion reside in an outer layer surrounding a central neuropil. There are six packets of neuronal somata in each segmental ganglion, and these are enveloped by six giant glial cells and separated by septa (48). In addition, two giant glial cells that extend multiple processes are present in the neuropil, and other giant glia cells envelop axons in the interganglionic connectives as well as the root nerves that extend from the ganglia to the bodywall. In the CNS, neurohemerythrin expression was detected in the giant glial cells in both the head (Fig. 4, *a–e*) and segmental ganglia (Fig. 4, *g–j*). Neuropile glial cells (Fig. 4, *a–e* and *g–j*), packet glial cells (Fig. 4*j*), and connective nerve glial cells (Fig. 4*f*) all contained hemerythrin mRNA. Blood vessel wall cells (Fig. 5, *a* and *b*), muscle cells (Fig. 5, *c* and *d*), and cells in the nephridia (Fig. 5, *e* and *f*) also showed hemerythrin mRNA expression.

We also assessed the presence of neurohemerythrin protein in the CNS by means of immunocytochemistry. Positive cells were observed in both the ganglia and the connective nerves. In ganglia, strong immunolabeling surrounded neuronal perikarya, but no signal was detected within the neurons, indicating that in the packets, only the glial cells expressed neurohemerythrin (Fig. 6, *a* and *b*). Hemerythrin immunoreactivity in the neuropile appeared to be restricted to glial cells as well (Fig. 6, *c* and *d*). In the connective nerves, strong signal was evident in the central region and in the outer layer in either

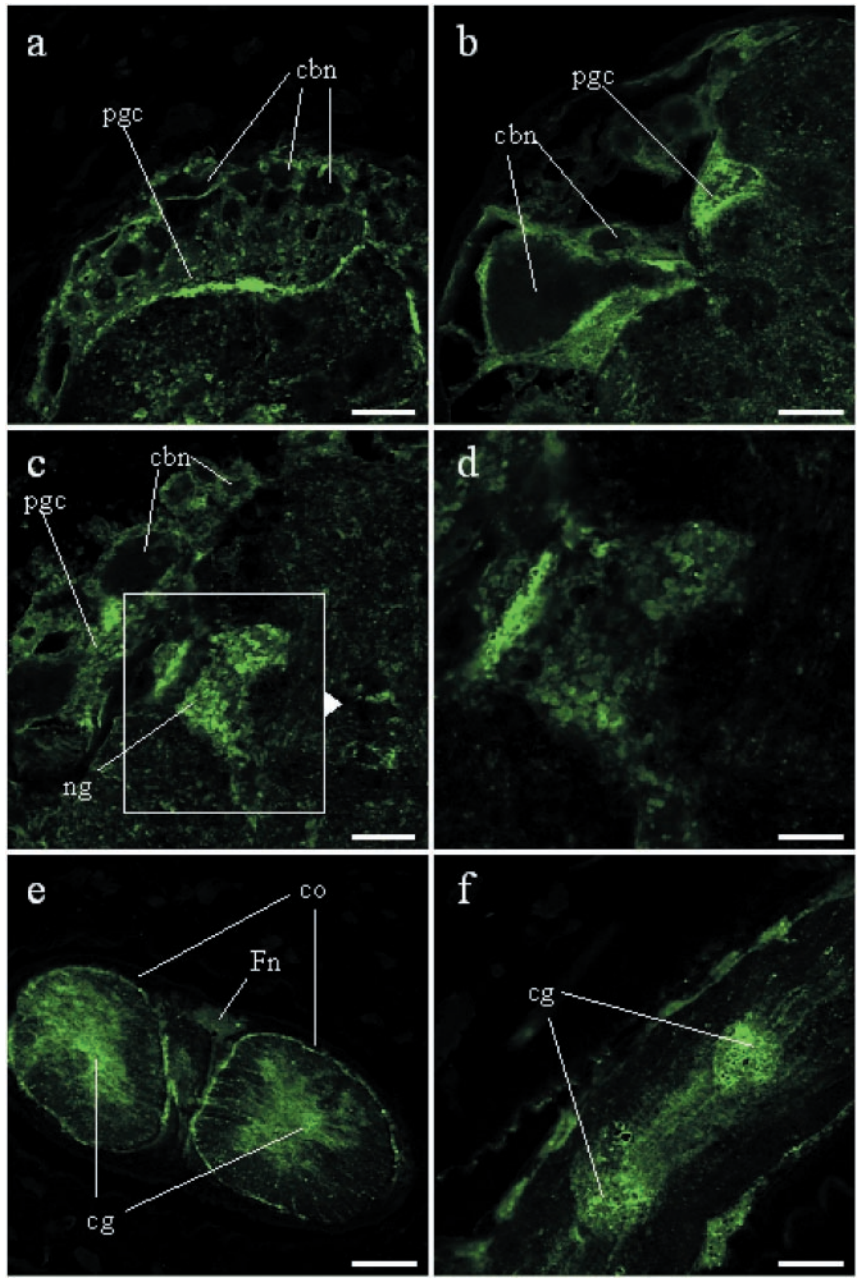


FIG. 6. **Immunodetection of hemerythrin in the CNS of *H. medicinalis*.** Positive cells are packet (*a*, *b*) and neuropile (*c*, *d*) glial cells within segmental ganglia and connective glial cells in the nerves between central ganglia (*e*, transversal section of connective; *f*, longitudinal section of connective). *cbn*, negatives of cell bodies of neurons; *cg*, connective glia; *co*, surfaces of connective nerves, *Fn*, negative of Faivre's nerve; *ng*, neuropile glia; *pgc*, packet glial cells. *Scale bars*: 10 $\mu$m (*a* and *c*), 2 $\mu$m (*b* and *d*) and 100 $\mu$m (*e* and *f*).

transversal or longitudinal sections of nerves (Fig. 6, *e* and *f*), corresponding to the connective glia that envelops axon fascicles and surrounding both connectives.

## DISCUSSION

The nervous system of the leech *H. medicinalis* responds to septic challenge, as shown here, with detectable changes in its expression of specific proteins. In particular, using a variety of approaches, we have shown that the expression of a protein annotated as 11/3 in two-dimensional gels (see Fig. 1) increased significantly after sepsis. Characterization tools, such as Edman degradation, cloning, and mass spectrometry, allowed us to obtain the entire coding sequence of the modulated 11/3 protein. Its sequence shows a high level of similarity to proteins belonging to the hemerythrin family. The degree of amino acid identity is much greater in the end regions: the protein shows 79% identity in the first 33 amino acid residues at the $NH_2$ terminus and 90% identity in the last 20 amino acid residues at the COOH terminus with hemerythrins of others annelids (Fig. 2*B*). Hemerythrins, which have been found thus far in four invertebrate phyla (sipunculids, priapulids, brachiopods, and annelids), are non-heme-iron oxygen-transport proteins whose oxygen binding properties via two iron atoms have been described (49).

Hemerythrins have been identified not only in circulating fluids as multisubunit forms assembled into octomers (up to aggregates of 690 kDa in the polychaete *Magelona papillicornis* (50), for example) but also in muscles as monomeric forms of 13–17 kDa (51). They have been described in body fluids, such as the coelomic fluid of *Phascolopis gouldi* (52), *Dendrostomum pyroides* (53), *Sipunculus nudus* (49), or *N. diversicolor* (54) and also, recently, in the regenerative Retzius' neurons of the leech *H. medicinalis* (55). However, using *in situ* hybridization, we were able to localize hemerythrin expression in the leech nerve cord to the giant neuropil, packet, and connective glial cells (Fig. 4) but not to neurons as do Blackshaw *et al.* (55). The giant neuropil glial cells have many branching processes that envelop the neurites of central neurons and the afferents of peripheral neurons.

These three glial cell types are electrically and dye coupled with each other by gap junctions (56, 57). In all nervous systems, glial cells are implicated in nervous tissue homeostasis (58, 59). They allow cellular nutrition of neurons and neuroprotection of the tissue. Farr *et al*. (60) have shown that inflammation causes hyperexcitability of sensory neurons of the mollusc *Aplysia californica*. Moreover, an oxygen supply is necessary for the transmission of impulses in neurons. In fact, the molluscan nerves failed to transmit impulses when placed in nitrogen or when the hemoglobin function is blocked by carbon monoxide (61, 62). The neurons oxygen-supplying role of oxygen-transport proteins is crucial for both the normal and stress situation. As an oxygen-binding molecule, a possible role for hemerythrin in an innate immune response we demonstrate here could be oxygen providing.

The work of Hunt (63) has assessed that normal well oxygenated tissues are highly resistant to infection. Bacterial challenge induced actually a stress response that involves metabolic needs. Oxygen providing to tissues, and particularly to nervous tissue, will satisfy these needs and allow an immune response of sufficient scale. Oxygen binding properties of hemerythrin via two iron atoms have been described (49). Hemerythrin is not the only oxygen-transport protein of the medicinal leech. Unlike other achaete Annelids, *H. medicinalis* has a closed circulatory system containing blood-carrying oxygen with hemoglobin (64). But to our knowledge, hemoglobin is located in blood vessels, and there are no myoglobin-like proteins to keep oxygen in organs and tissues, which have important needs in oxygen as muscles. Hemerythrin could perform this role. Indeed, hemerythrin has been found in Annelids muscles (51). In this work, we confirm this muscular localization in the medicinal leech. Moreover, we have also found hemerythrin in nephridia, which, as an excretory organ, also needs a high metabolic level. Finally, the presence of hemerythrin in blood vessel walls could be a link between the hemoglobin of the circulatory system and the hemerythrin in organs. We propose here that, in *H. medicinalis*, hemerythrin could take over the oxygen from the circulating hemoglobin to differents organs.

Another hypothetical role of hemerythrin in innate immunity of the leech could be antibacterial activity. Indeed, recent works from Deloffre *et al*. (65) showed that a hemerythrin-like peptide (MPII) isolated from the Annelid *N. diversicolor* was released in the blood stream after infection and possess a bacteriostatic activity. In this case, the hemerythrin expression in nephridial tissue would be important in Annelids because invading microorganisms can be excreted by nephridia (66) or engulfed by cells of the nephrostome (67). Expression of a bacteriostatic molecule, like hemerythrin, in this bacteria entrance/exit site would be crucial for the leech immunity. Moreover, as an iron-containing molecule, hemerythrin, could be involved in the iron availability regulation. Iron is a nutrient required for nearly all living organisms. Adequate iron storage proteins are also important for the defense of the organism against, first, the toxicity of membrane-destroying free radicals formed from ionic iron and, second, bacterial invasion. It has been shown, on the one hand, that the presence of free iron abolishes both bactericidal and bacteriostatic effects of diverse biological fluids like serum (68) or amniotic fluid (69) or of antibiotics (70) and leads to greatly enhanced virulence with increased rates of multiplication that can overwhelm natural defenses and, on the other hand, that iron-chelating resin reduces bacterial growth (71). Numerous proteins have iron-binding properties, but not all of them shielded iron from use by bacteria. Indeed, the other non-heme-iron protein transferrin captures iron and prevents its availability to the bacteria (72). Transferrin expression is up-regulated after *E. coli* infection of insects (73–76), while several studies have shown that heme compounds, like hemoglobin, possess virulence-enhancing properties with bacteria (77). As a non-heme iron protein, hemerythrin could act as transferrin in preventing free iron becoming available to bacteria. In this case, hemerythrin would compete with molecules as siderophores produced by bacteria to chelate iron from infected organism and would have indirect antibacterial properties.

On top of a role of hemerythrin in oxygen providing and iron availability regulation, we could not exclude a role of hemerythrin as bioactive peptide precursor. Indeed, several Invertebrates are able to generate, from oxygen-carrying molecules like hemoglobin or hemocyanin, peptides presenting pleiotropic activities like antimicrobial (78, 79) or neuropeptidic (80, 81) like Vertebrates (82).

In conclusion, we report here the implication of neurohemerythrin in innate immunity of the leech nervous system thanks to its increased representativity on two-dimensional gels after bacterial challenge and its expression by central nervous system glial cells. Its exact role in neuroprotection remains to be detailed, but we propose here a double role of hemerythrin in innate immunity: a role in oxygen providing to satisfy metabolic needs induced by bacterial challenge and a role in the regulation of free iron availibility to deprive bacteria of iron essential for their growth.

*Acknowledgments*—We thank Annie Desmons for her skilled technical assistance and Eric Décout from Proteaxis (Loos, France) for allowing and helping us to use the Progenesis™ software.

REFERENCES

1. Kakizaki, Y., Watanobe, H., Kohsaka, A., and Suda, T. (1999) *Endocr. J.* **46,** 487–496
2. Rivest, S., Lacroix, S., Vallieres, L., Nadeau, S., Zhang, J., and Laflamme, N. (2000) *Proc. Soc. Exp. Biol. Med.* **223,** 22–38
3. Hoffmann, J. A., Kafatos, F. C., Janeway, C. A., and Ezekowitz, R. A. (1999) *Science* **284,** 1313–1318
4. Janeway, C. A., Jr., and Medzhitov, R. (2002) *Annu. Rev. Immunol.* **20,** 197–216
5. Khush, R. S., and Lemaitre, B. (2000) *Trends Genet.* **16,** 442–449
6. Lemaitre, B., Reichhart, J. M., and Hoffmann, J. A. (1997) *Proc. Natl. Acad. Sci. U. S. A.* **94,** 14614–14619
7. Zasloff, M. (2002) *Nature* **415,** 389–395
8. Anderson, R. S. (2001) *Adv. Exp. Med. Biol.* **484,** 131–139
9. De Gregorio, E., Spellman, P. T., Rubin, G. M., and Lemaitre, B. (2001) *Proc. Natl. Acad. Sci. U. S. A.* **98,** 12590–12595
10. Iwanaga, S., Kawabata, S., and Muta, T. (1998) *J. Biochem. (Tokyo)* **123,** 1–15
11. Hall, M., Wang, R., van Antwerpen, R., Sottrup-Jensen, L., and Soderhall, K. (1999) *Proc. Natl. Acad. Sci. U. S. A.* **96,** 1965–1970
12. Soderhall, K., and Cerenius, L. (1998) *Curr. Opin. Immunol.* **10,** 23–28
13. Mitta, G., Vandenbulcke, F., and Roch, P. (2000) *FEBS Lett.* **486,** 185–190
14. Miller, J. S., Nguyen, T., and Stanley-Samuelson, D. W. (1994) *Proc. Natl. Acad. Sci. U. S. A.* **91,** 12418–12422
15. Pech, L. L., and Strand, M. R. (1996) *J. Cell Sci.* **109,** 2053–2060
16. Hoffmann, J. A., and Reichhart, J. M. (2002) *Nat. Immunol.* **3,** 121–126
17. Pace, K. E., Lebestky, T., Hummel, T., Arnoux, P., Kwan, K., and Baum, L. G. (2002) *J. Biol. Chem.* **277,** 13091–13098
18. Cantera, R., Roos, E., and Engstrom, Y. (1999) *J. Neurobiol.* **38,** 16–26
19. Preiss, A., Johannes, B., Nagel, A. C., Maier, D., Peters, N., and Wajant, H. (2001) *Mech. Dev.* **100,** 109–113
20. Pujol, N., Link, E. M., Liu, L. X., Kurz, C. L., Alloing, G., Tan, M. W., Ray, K. P., Solari, R., Johnson, C. D., and Ewbank, J. J. (2001) *Curr. Biol.* **11,** 809–821
21. Lassegues, M., Milochau, A., Doignon, F., Du Pasquier, L., and Valembois, P. (1997) *Eur. J. Biochem.* **246,** 756–762
22. Bilej, M., De Baetselier, P., Van Dijck, E., Stijlemans, B., Colige, A., and Beschin, A. (2001) *J. Biol. Chem.* **276,** 45840–45847
23. Salzet, M., Wattez, C., and Slomianny, M. C. (1993) *Comp. Biochem. Physiol. Comp. Physiol.* **104,** 75–81
24. Laurent, V., Salzet, B., Verger-Bocquet, M., Bernet, F., and Salzet, M. (2000) *Eur. J. Biochem.* **267,** 2354–2361
25. Retzius, G. (1891) *Biologische Untersuchengen, Neue Folge*, Vol. 2, pp. 1–28, Samson and Wallin, Stockholm, Sweden
26. Ehrenberg, C. G. (1836) *Beobachtungen einer auffallenden bisher unbekannten Structur des Seelenorgans bei Menschen und Thieren*, Koenigliche Akademie der Wissenschaften, Berlin
27. Macagno, E. R. (1980) *J. Comp. Neurol.* **190,** 283–302
28. Macagno, E. R., Peinado, A., and Stewart, R. R. (1986) *Proc. Natl. Acad. Sci. U. S. A.* **83,** 2746–2750
29. Xie, Y., Yeo, T. T., Zhang, C., Yang, T., Tisi, M. A., Massa, S. M., and Longo, F. M. (2001) *J. Neurosci.* **21,** 5130–5138

30. Emes, R. D., Wang, W. Z., Lanary, K., and Blackshaw, S. E. (2003) *FEBS Lett.* **533,** 124–128
31. Korneev, S., Fedorov, A., Collins, R., Blackshaw, S. E., and Davies, J. A. (1997) *Invertebr. Neurosci.* **3,** 185–192
32. Damerval, C., De Vienne, D., Zivy, M., and Thiellement, H. (1986) *Electrophoresis* **7,** 52–54
33. Peterson, G. L. (1977) *Anal. Biochem.* **83,** 346–356
34. Wu, X., Ritter, B., Schlattjan, J. H., Lessmann, V., Heumann, R., and Dietzel, I. D. (2000) *J. Neurobiol.* **44,** 320–332
35. Schägger, H., and von Jagow, G. (1987) *Anal. Biochem.* **166,** 368–379
36. Morrissey, J. H. (1981) *Anal. Biochem.* **117,** 307–310
37. Neuhoff, V., Arold, N., Taube, D., and Ehrhardt, W. (1988) *Electrophoresis* **9,** 255–262
38. Shaw, C., Thim, L., and Conlon, J. M. (1987) *J. Neurochem.* **49,** 1348–1354
39. Mackey, A. J., Haystead, T. A., and Pearson, W. R. (2002) *Mol. Cell. Proteomics* **1,** 139–147
40. Rajeevan, M. S., Ranamukhaarachchi, D. G., Vernon, S. D., and Unger, E. R. (2001) *Methods* **25,** 443–451
41. Pfaffl, M. W. (2001) *Nucleic Acids Res.* **29,** e45
42. Mitta, G., Vandenbulcke, F., Noel, T., Romestand, B., Beauvillain, J. C., Salzet, M., and Roch, P. (2000) *J. Cell Sci.* **113,** 2759–2769
43. Munoz, M., Vandenbulcke, F., Saulnier, D., and Bachere, E. (2002) *Eur. J. Biochem.* **269,** 2678–2689
44. Demuynck, S., Li, K. W., Van der Schors, R., and Dhainaut-Courtois, N. (1993) *Eur. J. Biochem.* **217,** 151–156
45. Coutte, L., Slomianny, M. C., Malecha, J., and Baert, J. L. (2001) *Biochim. Biophys. Acta* **1518,** 282–286
46. Hendrickson, W. A., Klippenstein, G. L., and Ward, K. B. (1975) *Proc. Natl. Acad. Sci. U. S. A.* **72,** 2160–2164
47. Stenkamp, R. E., Sieker, L. C., Jensen, L. H., McCallum, J. D., and Sanders-Loehr, J. (1985) *Proc. Natl. Acad. Sci. U. S. A.* **82,** 713–716
48. Coggeshall, R. E., and Fawcett, D. W. (1964) *J. Neurophysiol.* **27,** 229–289
49. Bates, G., Brunori, M., Amiconi, G., Antonini, E., and Wyman, J. (1968) *Biochemistry* **7,** 3016–3020
50. Manwell, C., and Baker, C. M. A. (1988) *Comp. Biochem. Physiol. B* **89,** 453–463
51. Klippenstein, G. L., Van Riper, D. A., and Oosterom, E. A. (1972) *J. Biol. Chem.* **247,** 5959–5963
52. Mangum, C. P., and Kondon, M. (1975) *Comp. Biochem. Physiol. A* **50,** 777–785
53. Ferrell, R. E., and Kitto, G. B. (1970) *Biochemistry* **9,** 3053–3058
54. Demuynck, S., Sautiere, P., van Beeumen, J., and Dhainaut-Courtois, N. (1991) *C. R. Acad. Sci. III* **312,** 317–322
55. Blackshaw, S. E., Babington, E. J., Emes, R. D., Malek, J., and Wang, W. Z. (2004) *J. Anat.* **204,** 13–24
56. Coggeshall, R. E. (1974) *J. Neurobiol.* **5,** 463–467
57. Lohr, C., and Deitmer, J. W. (1997) *Exp. Biol. Online* **2,** 8
58. Deitmer, J. W. (2001) *Respir. Physiol.* **129,** 71–81
59. Streit, W. J. (2000) *Toxicol. Pathol.* **28,** 28–30
60. Farr, M., Mathews, J., Zhu, D. F., and Ambron, R. T. (1999) *Learn Mem.* (*Cold Spring Harb.*) **6,** 331–340
61. Kraus, D. W., and Colacino, J. M. (1986) *Science* **232,** 90–92
62. Kraus, D. W., and Doeller, J. E. (1988) *Biol. Bull.* **174,** 346–354
63. Hunt, T. K. (1988) *Ann. Emerg. Med.* **17,** 1265–1273
64. Ilan, E., and Haroun, J. (1993) *Biochim. Biophys. Acta* **1162,** 77–83
65. Deloffre, L., Salzet, B., Vieau, D., and Salzet, M. (2003) *Neuroendocrinol. Lett.* **24,** 40–45
66. Cameron, G. R. (1932) *J. Pathol.* **35,** 933–972
67. Villaro, A. C., Sesma, P., Alegria, D., Vazquez, J. J., and Lopez, J. (1985) *J. Morphol.* **186,** 307–314
68. Rogers, H. J. (1976) *Immunology* **30,** 425–433
69. Oka, K., Hagio, Y., Tetsuoh, M., Kawano, K., Hamada, T., and Kato, T. (1987) *Biol. Res. Pregnancy Perinatol.* **8,** 1–6
70. Okamoto, R., Hara, T., Yoshida, T., Orikasa, Y., Ogino, H., Iwamatsu, K., and Inouye, S. (1990) *Drugs Exp. Clin. Res.* **16,** 157–165
71. Feng, M., van der Does, L., and Bantjes, A. (1994) *J. Med. Chem.* **37,** 924–927
72. Valenti, P., Antonini, G., Von Hunolstein, C., Visca, P., Orsi, N., and Antonini, E. (1983) *Int. J. Tissue React.* **5,** 97–105
73. Yoshiga, T., Georgieva, T., Dunkov, B. C., Harizanova, N., Ralchev, K., and Law, J. H. (1999) *Eur. J. Biochem.* **260,** 414–420
74. Yoshiga, T., Hernandez, V. P., Fallon, A. M., and Law, J. H. (1997) *Proc. Natl. Acad. Sci. U. S. A.* **94,** 12337–12342
75. Seitz, V., Clermont, A., Wedde, M., Hummel, M., Vilcinskas, A., Schlatterer, K., and Podsiadlowski, L. (2003) *Dev. Comp. Immunol.* **27,** 207–215
76. Thompson, G. J., Crozier, Y. C., and Crozier, R. H. (2003) *Insect Mol. Biol.* **12,** 1–7
77. Ward, C. G., Hammond, J. S., and Bullen, J. J. (1986) *Infect. Immun.* **51,** 723–730
78. Fogaca, A. C., da Silva, P. I., Jr., Miranda, M. T., Bianchi, A. G., Miranda, A., Ribolla, P. E., and Daffre, S. (1999) *J. Biol. Chem.* **274,** 25330–25334
79. Destoumieux-Garzon, D., Saulnier, D., Garnier, J., Jouffrey, C., Bulet, P., and Bachere, E. (2001) *J. Biol. Chem.* **276,** 47070–47077
80. Salzet, M., and Deloffre, L. (2000) *Curr. Trends Immunol.* **3,** 151–156
81. Salzet, M., Bulet, P., Weber, W. M., Clauss, W., Verger-Bocquet, M., and Malecha, J. (1996) *J. Biol. Chem.* **271,** 7237–7243
82. Ivanov, V. T., Karelin, A. A., Philippova, M. M., Nazimov, I. V., and Pletnev, V. Z. (1997) *Biopolymers* **43,** 171–188